Fault Estimation and Monitoring with Multi-Sensor Data Fusion: An Unscented Kalman Filter Approach

Abstract— In this paper, an unscented Kalman filter (UKF) is proposed in an integrated design frameworks to utilize multi-sensor data fusion techniques for process fault monitoring. The multi-sensor data fusion (MSDF) technique is presented by frameworks of centralized and decentralized architectures. A set of simulation studies has been conducted to demonstrate the performance of the proposed scheme on quadruple tank system (QTS) and industrial utility boiler (IUB). It is established that the decentralized integrated framework retrieves more effectively the critical information about presence or absence of a fault from the dynamic model with minimum time delay and provides accurate unfolding-in-time of the finer details of the fault as compared to the centralized integrated framework, thus completing the overall picture of fault monitoring of the system under test. Experimental results on QTS and IUB, show that the proposed method is able to correctly identify various faults even when the dynamics of the systems are large.

Index Terms— Fault monitoring, fault estimation, unscented Kalman filter, integrated design framework, multi-sensor data fusion, quadruple tank system, industrial utility boiler.

Nomenclature

Table I shows the variables used in the paper.

I. Introduction

THE problem of fault monitoring has always been an area of much importance for the research departments in the industries. And this importance become more prioritized when we are dealing with the non-linear systems. Monitoring of uncommon behavior of the plants and detecting the unprecedented changes in system are the essential steps to maintain the health of the system, followed by covering the removal of faulty components, replacement with the better ones, restructuring system architecture, and thus improving the overall system reliability. However, with the increasing complexity of the modern nonlinear systems, process engineers are facing tough challenges to understand and trouble-shoot possible system problems [1]. Further recent applications are found in [2]–[8]. Therefore due to the large system structure, highly efficient fault monitoring methods have become a valuable asset for the life of the systems.

Failures can be classified as sudden or incipient. Sudden failures are often the simplest form to diagnose since they usually have a dramatic impact on performance, which can be detected at a number of downstream sensors. When

a blast occurs, the impact can be felt everywhere in the vicinity. However, incipient or gradual failures are difficult to detect since they manifest themselves as a slow degradation in performance which can only be detected over time. The techniques which are based on identifying

TABLE I
NOMENCLATURE

Symbols	Function
$\bar{x}$	mean
P_x	covariance
$2L+1$	Sigma vectors in UKF
QTS	acronym for quadruple tank System
IUB	acronym for industrial utility boiler
UT	acronym for Unscented transformation
α	Spread of the sigma points around $\bar{x}$
κ	Secondary scaling parameter
$\mathbf{x}$	random variable (dimension L)
β	incorporate prior knowledge of the dstrb. of $\mathbf{x}$
λ	Composite scaling parameter
L	Dimension of the augmented state
R^v	Process-noise covariance
R^n	Measurement-noise covariance
W_i	weights
$\mathbf{w}_k$	Stationary process with identity state transition matrix
r_k	Noise
d_k	desired output
w_k	non-linear observation
R^e	constant diagonal matrix
λ_{RLS}	forgetting factor
h_i	Level of water in tank i in QTS
a_i	Area of water flowing out from tank i in QTS
A_i	Area of tank i
γ_1	tank 1 and tank 4 water diverting ration in QTS
γ_2	tank 2 and tank 3 water diverting ration in QTS
k_1	Gain of Pump 1 in QTS
k_2	Gain of Pump 2 in QTS
ν_1	Manipulated input 1 (pump 1) in QTS
ν_2	Manipulated input 2 (pump 2) in QTS
g	Gravitational constant in QTS
a_{leak1}	Leak in pipe of tank 1 in QTS
a_{leak2}	Leak in pipe of tank 2 in QTS
a_{leak3}	Leak in pipe of tank 3 in QTS
a_{leak4}	Leak in pipe of tank 4 in QTS
q_{in}	inflow in QTS
q_{out}	outflow in QTS
u_1	feed water flow rate (kg/s) in IUB
u_2	fuel flow rate (kg/s) in IUB
u_3	at temperator spray flow rate (kg/s) in IUB
y_1	drum level (m) in IUB
y_2	drum pressure kPa in IUB
y_3	steam temperature C^0 in IUB
x_2	Upstream pressure in IUB
P_{header}	Downstream pressure in IUB
x_1	fluid density of the system in IUB
V_T	Total volume of the system in IUB

a model and using performance or error metrics to detect failure will find it difficult to identify a failure which occurs at a rate slower (often, much slower) than the model drifts under normal conditions. It should be noted here that there is another class of failure which has largely been ignored in the fault detection literature is a 'pre-existing' failure. This is because a model of correct operation is impossible to identify simply by looking at a unit after it has already failed, and so most practical fault detection techniques are simply inapplicable to this type of fault. Some recent papers on the same or similar topic have been published in [9]-[13] where modified Kalman filters have been used for various applications such as green house climate control, chaos systems, estimation problems etc. Most recent approaches for fault monitoring and detection can be found in [14]-[17].

In this paper, a UKF has been proposed in an integrated design framework to utilize MSDF techniques for process fault monitoring, thus completing a picture of a new automated fault detection and diagnosis system based on an enhanced UKF estimator. The proposed methodology utilizes a MSDF technique to enhance the accuracy and reliability of parametric estimation in the process fault detection. This technique seeks to combine data from multiple sensors and related information to achieve improved accuracies and more specific inferences. The technique encapsulates the UKF in centralized and decentralized architectures for MSDF promoting to an improved fault monitoring. The extended Kalman filter (EKF) based centralized and decentralized fault monitoring MSDF was originally proposed for a continuous time stirred tank reactor problem in [18] . We use a similar approach where a UKF is used to detect the presence or absence of a fault. The proposed scheme has then been successfully evaluated on a QTS and an IUB, thus corroborating the theory underpinning it.

The paper is organized as follows: in Section II the related work is presented. Problem formulation is presented in Section III. In Section IV, first, the UKF has been presented, then the integration of the UKF with centralized and decentralized architectures of MSDF has been presented, followed by the evaluation of the proposed scheme in section V. Section VI presents the simulation results for the technique implemented. Finally some concluding remarks are given in Section VII.

II. RELATED WORKS

This section contains the related work which has been conducted in this area of performance monitoring of plants: model based schemes for fault detection, model-free schemes for fault detection, and probabilistic models with fault detection.

II.A. Model-Based Schemes

The model-based approach is popular for developing fault detection and isolation (FDI) techniques [19]. It

mainly consists of two stages [20]. The first one is to generate residuals by computing the difference between the measured output from the system and the estimated output obtained from the state system estimator used (e.g Kalman Filter). Any departure from zero of the residuals indicates a fault has likely occurred [21]. However, these methods are developed mainly for linear systems assuming that a precise mathematical model of the system is available. This assumption, however, may be difficult to satisfy in practice, especially as engineering systems in general are nonlinear and are becoming more complex [22]. [23] has done a work of integration of industrial system techniques with the development of model-based adaptive control charts for quality monitoring.

II.B. Model-Free Schemes

For model-free approaches, only the availability of a large amount of historical process data is assumed. There are different ways in which this data can be transformed and presented as a-priori knowledge to a diagnostic system. This is known as the feature extraction process from the process history data, and it is done to facilitate later diagnosis [24]. This extraction process can proceed mainly as either a quantitative or a qualitative feature extraction process. Quantitative feature extraction can be either statistical or non-statistical. Model-Free techniques such as neural networks, fuzzy logic and genetic algorithms are used to develop models for FDI techniques. These models not only can represent a wide class of nonlinear systems with arbitrary accuracy, they can also be trained from data. Among these techniques, neural networks are well recognized for their ability to approximate nonlinear functions and for their learning ability [25]. For these reasons, they have been used as models to generate residuals for fault detection [26]–[30]. However, it is very difficult to isolate faults with these networks as they are black boxes in nature. Further, it is also desirable that fault diagnostic system should be able to incorporate the experience of the operators [31]. Fuzzy reasoning allows symbolic generalization of numerical data by fuzzy rules and supports the direct integration of the experience of the operators in the decision making process of FDI in order to achieve more reliable fault diagnosis [32]–[33]. A rule-based expert system for fault diagnosis in a cracker unit is described in [34]. Optimization algorithms such as genetic algorithm and particle swarm optimization that simulate biological processes to solve search and optimization problems are also implemented to have a better pictorial view of fault detection and even classification.

II.C. Probabilistic Schemes

Bayesian belief networks provide a probabilistic approach to consider cause-and-effect relation between process variables. There have been a few attempts to apply Bayesian belief networks for fault detection and diagnosis. [35] has worked in probabilistic sensor fault detection

and identification. [36] proposed an approach to present a Bayesian belief networks model in the form of a set of nonlinear equations and constraints that should be solved for the unknown probabilities. As an inference tool, [37] used genetic algorithm for fault diagnosis in a Bayesian belief networks representing a fluid catalytic cracking process. [38] used the learning capability of Bayesian belief networks to use process data in an adaptable fault diagnosis strategy. Bayesian belief networks are also used to perform fault detection and diagnosis for discrete events like walking [39] and [40]. Probabilistic approach with application to bearing fault-detection is also implemented in [41].

To express the problem statement, fault is an undesirable factor in any process control industry. It affects the efficiency of the system operation and reduces economic benefits to the industry. The early detection and diagnosis of faults in mission critical systems becomes highly crucial for preventing failure of equipment, loss of productivity and profits, management of assets, reduction of shutdowns.

III. PROBLEM FORMULATION

To have an effective fault diagnosis approach of highly nonlinear systems, we have assumed various faults in the system which have been successfully monitored and estimated through the encapsulation of the UKF in various architectures of multi-data fusion technique. Fig. 1 shows the proposed scheme has been introduced here by showing the implementation plan of fault monitoring using UKF. Assume that a process is monitored by N different sensors, described by the following general nonlinear process and measurement models in discrete time state-space framework:

$$
\begin{aligned}
x(k) &= f(x(k-1), u(k-1), d(k-1)) + w(k-1) \\
z_i &= h_i(x(k)) + \nu_i(k); \quad i = 1, ..., N
\end{aligned}
\tag{1}
$$

where $f(.)$ and $h_i(.)$ are the known nonlinear functions, representing the state transition model and the measurement model, respectively. $x(k) \in R_{n_x}$ is the process state-vector, $u(k) \in R_{n_u}$ denotes the manipulated process variables, $d(k) \in R_{n_d}$ represents the process faults modeled by the process disturbances, $z_i(k) \in R_{n_{zi}}$ are the measured variables obtained from the N installed sensors, $w(k)$ and $v_i(k)$ indicate the stochastic process and measurement disturbances modeled by zero-mean white Gaussian noises with covariance matrices $Q(k)$ and $R_i(k)$, respectively.

III.A. Discrete time UKF

In most practical applications of interest, the process and/or measurement dynamic models are described by nonlinear equations, represented in the system (1). This means that the non-linear behavior can affect the process operation at least through its own process dynamics

or measurement equation. In such cases, the standard Kalman filter algorithm is often unsuitable to estimate the process states using its linearized time-invariant state-space model at the desired process nominal operating point. UKF gives a simple and effective remedy to overcome such nonlinear estimation problem. Its basic idea is to locally linearize the nonlinear functions, described by system (1), at each sampling time instant around the most recent process condition estimate. This allows the Kalman filter to be applied to the following linearized time varying model:

$$
\begin{aligned}
x(k) &= A(k)x(k-1) + B_u(k)u(k-1) + B_d(k) \\
&\quad d(k-1) + w(k-1) \\
z_i(k) &= H_i(k)x(k) + \nu_i(k); \quad i = 1, ..., N
\end{aligned}
\tag{2}
$$

where the state transition matrix $A(k)$, the input matrices $B_u(k)$ and $B_d(k)$, and the observation matrix $H_i(k)$ are the jacobian matrices which are evaluated at the most recent process operating condition in real-time rather than the process fixed nominal values:

$$
A(k) = \frac{\partial f}{\partial x}|_{\hat{x}(k)}
\tag{3}
$$

$$
B_u(k) = \frac{\partial f}{\partial u}|_{u(k)}
\tag{4}
$$

$$
B_d(k) = \frac{\partial f}{\partial d}|_{\hat{d}(k)}
\tag{5}
$$

$$
H_i(k) = \frac{\partial h_i}{\partial x}|_{\hat{x}(k)}, \quad i = 1, ..., 10
\tag{6}
$$

In classical control, disturbance variables $d(k)$ are treated as known inputs with distinct entry in the process state-space model. This distinction between state and disturbance as non-manipulated variables, however, is not justified from the monitoring perspective using the estimation procedure. Therefore, a new augmented state variable vector $x^*(k) = [d^T(k) \quad x^T(k)]^T$ is developed by considering the process disturbances or faults as additional state variables. To implement this view, the process faults are assumed to be random state variables governed by the following stochastic auto-regressive (AR) model equation:

$$
d(k) = d(k-1) + w_d(k-1)
\tag{7}
$$

This assumption changes the linearized model formulations in system (2) to the following augmented state-space model:

$$
\begin{aligned}
x^*(k) &= A^*(k)x^*(k-1) + B^*(k)u(k-1) + \\
&\quad w^*(k-1) \\
z_i(k) &= H_i^*(k)x^*(k) + \nu_i(k); \quad i = 1, ..., N
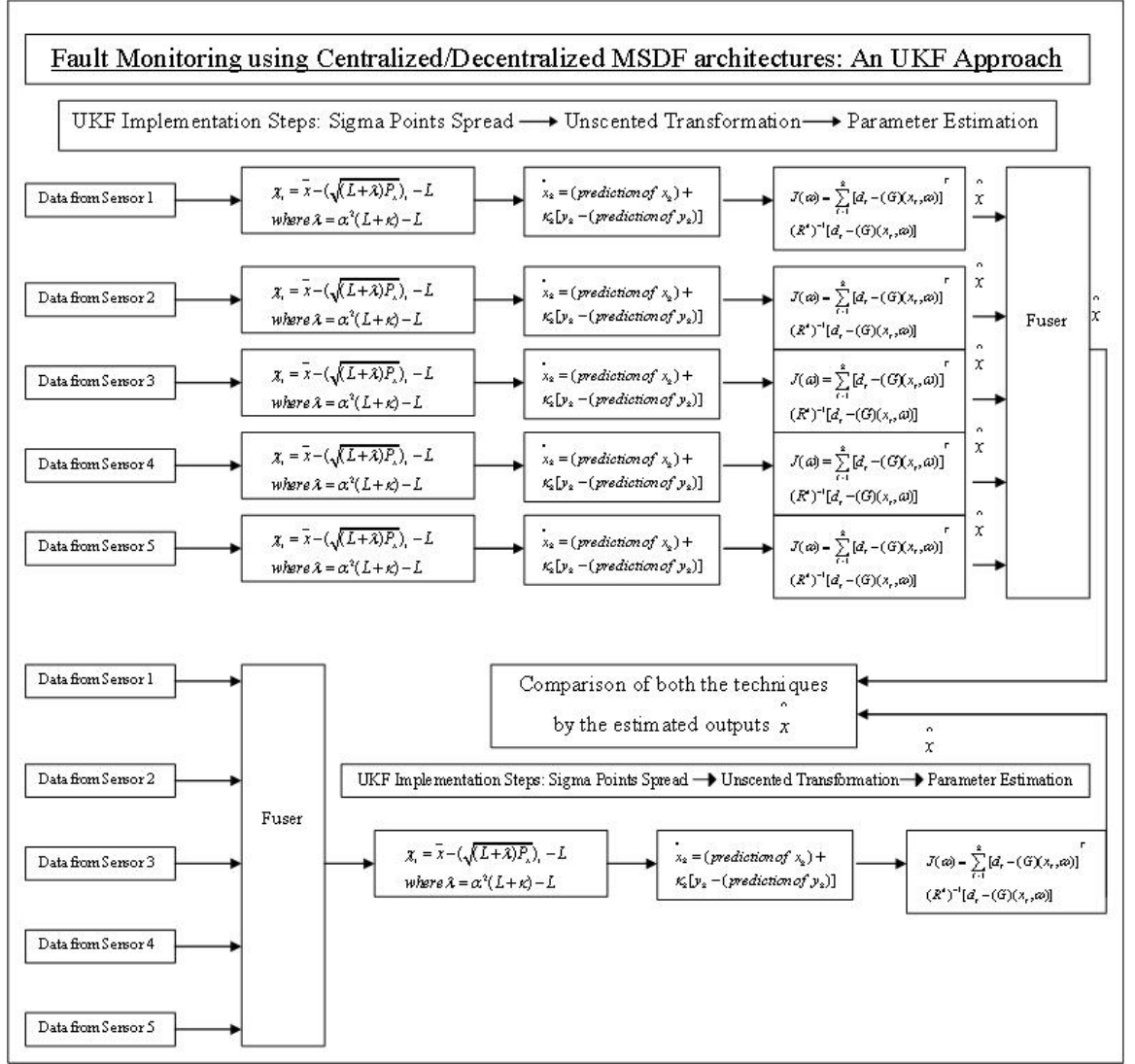\end{aligned}
\tag{8}
$$

Fig. 1. Implementation plan for the evaluation of the UKF-based proposed scheme

Noting that:

$$A^*(k) = \begin{bmatrix} I^{n_d \times n_d} & 0^{n_d \times n_x} \\ B_d(k)^{n_x \times n_d} & Ak^{n_x \times n_x} \end{bmatrix} \quad (9)$$

$$B^*(k) = \begin{bmatrix} 0^{n_d \times n_u} & B_u(k)^{n_x \times n_u} \end{bmatrix}^T \quad (10)$$

$$H_i^*(k) = \begin{bmatrix} 0^{1 \times n_d} & H_i(k)^{1 \times n_x} \end{bmatrix} \quad (11)$$

$$W^*(k-1) = \begin{bmatrix} w_d(k-1)^{n_d \times 1} & w(k-1)^{n_x \times 1} \end{bmatrix}^T \quad (12)$$

Assumption 3.1: There exists a known positive constant L_0 such that for any norm bounded $x_1(t), x_2(t) \in \mathbf{R}^n$, the following inequality holds:

$$\|f(u(k), y(k), x_1(k)) - f(u(k), y(k), x_2(k))\| \\ \leq L_0 \|x_1(k) - x_2(k)\| \quad (13)$$

Assumption 3.2: $C[sI - (A - KC)]^{-1}B$ is strictly positive real, where $K \in \mathbf{R}^{n \times r}$ is chosen such that $A - KC$ is stable.

Remark 3.1: For a given positive definite matrix $Q > 0 \in \mathbf{R}^{n \times n}$, there exists matrices $P = P^T > 0 \in \mathbf{R}^{n \times n}$ and a scalar R such that:

$$(A - KC)^T P + P(A - KC) = -Q \quad (14)$$
$$PB = C^T R \quad (15)$$

to detect the fault, the following is constructed:

$$\hat{x}(k) = A\hat{x}(k) + g(u(k), y(k)) + B\xi_H f(u(k), y(k),$$
$$\hat{x}(k)) + K(y(k) - \hat{y}(k)) \quad (16)$$
$$\hat{y}(k) = C\hat{x}(k) \quad (17)$$

where $\hat{x}(k) \in \mathbf{R}^n$ is the state estimate, the input is $u \in \mathbf{R}^m$, and the output is $y \in \mathbf{R}^r$. The pair (A, C) is observable. The non-linear term $g(u(k), y(k))$ depends on $u(k)$ and $y(k)$ which are directly available. The $f(u(k), y(k), x(k)) \in \mathbf{R}^r$ is a nonlinear vector function of $u(k)$, $y(k)$ and $x(k)$. The $\xi(k) \in \mathbf{R}$ is a parameter which changes unexpectedly when a fault occurs. Since it has been assumed that the pair (A, C) is observable, a gain matrix K can be selected such that $A - KC$ is a stable matrix. We define:

$$e_x(k) = x(t) - \hat{x}(k), \quad e_y(k) = y(k) - \hat{y}(k) (18)$$

Then, the error equations can be given by:

$$e_x(k+1) = (A - KC)e_x(k) + B[\xi(k)f(u(k), y(k),$$
$$x(k)) - \xi_H f(u(k), y(k), \hat{x}(k))], \quad (19)$$
$$e_y(k) = Ce_x(k) \quad (20)$$

The convergence of the above filter is guaranteed by the following theorem:

Theorem 3.1: Under the assumption (3.2), the filter is asymptotically convergent when no fault occurs $(\xi(k) = \xi_H)$,i.e. $lim_{k\to\infty} e_y(k) = 0$.

Proof: Consider the following Lyapunov function

$$V(e(k)) = e_x^T(k)Pe_x(k) \quad (21)$$

where P is given by the system (14), Q is chosen such that $\rho_1 = \lambda_{min}(Q) - 2\|C\|.|R|\xi_H L_0 > 0$ Along the trajectory of the fault-free system (19), the corresponding Lyapunov difference along the trajectories $e(k)$ is:

$$\Delta V = E\{V(e(k+1)|e_k, p_k)\} - V(e(k))$$
$$= E\{e^T(k+1)P_ie(k+1)\} - e^T(k)P_ie(k)$$
$$= (A_e e_x + B_L u_e)^T P(A_e e_x + B_L u_e)$$
$$- e_x^T(k)Pe_x(k)$$
$$= e^T(k)[(P(A - KC) + (A - KC)^T P)$$
$$+ PB\xi_H[f(u(k), y(k), x(k))$$
$$- f(u(k), y(k), \hat{x}(k))]]e(k) \quad (22)$$

From (3.1) and system (14), one can further obtain that

$$\Delta V \leq -e_x^T(k)Qe_x(t) + 2\|e_y(k)\|.|R|\xi_H L_0\|e_x(k)\|$$
$$\leq -\rho_1\|e_x\|^2 < 0 \quad (23)$$

Thus, $lim_{k\to\infty} e_x(k) = 0$ and $lim_{k\to\infty} e_y(k) = 0$. This completes the proof. ∎

The UKF essentially addresses the approximation issues of the extended Kalman filter (EKF) [42]–[44]. The basic difference between the EKF and UKF stems from the manner in which Gaussian random variables (GRV) is presented through system dynamics. In the EKF, the state distribution is approximated by GRV, which is then propagated analytically though the first-order linearization of the non-linear system. This can introduce large errors in the true posterior mean covariance of the transformed GRV, which may lead to sub-optimal performance and sometimes divergence of the filter. The UKF addresses this problem by using a deterministic sampling approach. The state distribution is again approximated by a GRV, but is now represented using a minimal set of carefully chosen sample points. These sample points completely capture the true mean and covariance of the GRV, and when propagated through the *true* non-linear system, capture the posterior mean and covariance accurately to second order (Taylor series expansion) for any nonlinearity. The EKF, in contrast, only achieves first-order accuracy (See remark 3.3 for details).

III.B. Unscented Transformation (UT)

The structure of the UKF is elaborated by UT for calculating the statistics of a random variable which undergoes a nonlinear transformation [44]. Consider propagating a random variable **x** (dimension L) through a nonlinear function, $y = f(x)$. Assume **x** has mean $\bar{x}$ and covariance P_x. To calculate the statistics of y, we form a matrix $\mathcal{X}$ of $2L + 1$ sigma vectors $\mathcal{X}_i$ according to:

$$\mathcal{X}_0 = \bar{x},$$
$$\mathcal{X}_i = \bar{x} + (\sqrt{(L+\lambda)\mathbf{P_x}})_i, \quad i = 1, .., L$$
$$\mathcal{X}_i = \bar{x} - (\sqrt{(L+\lambda)\mathbf{P_x}})_i - L, \quad i = L+1, .., 2L$$
$$(24)$$

where $\lambda = \alpha^2(L + \kappa) - L$ is a scaling parameter. The constant α determines the spread of the sigma points around $\bar{x}$, and is usually set to a small positive value $(1 \leq \alpha \leq 10^{-4})$. The constant κ is a secondary scaling parameter, which is usually set to $3 - L$, and β is used to incorporate prior knowledge of the distribution of **x** (for Gaussian distributions, $\beta = 2$) is optimal). $(\sqrt{(L+\lambda)\mathbf{P_x}})_i$ is the ith column of the matrix square root (that is, lower-triangular Cholesky factorization). These sigma vectors are propagated through the nonlinear function $\mathcal{Y}_i = f(\mathcal{X}_i), i = 0, ..., 2L$. Now the mean and covariance for y are approximated using a weighted sample mean and covariance of the posterior sigma points:

$$\bar{y} \approx \sum_{i=0}^{2L} W_i^m \mathcal{Y}_i,$$

$$\mathbf{P}_y \approx \sum_{i=0}^{2L} W_i^c (\mathcal{Y}_i - \bar{y})(\mathcal{Y}_i - \bar{y})^T,$$

$$W_0^{(m)} = \frac{\lambda}{L + \lambda},$$

$$W_0^{(c)} = \frac{\lambda}{L + \lambda} + 1 - \alpha^2 + \beta,$$

$$W_i^{(m)} = W_i^{(c)} = \frac{1}{2(L+\lambda)}, i = 1, ..., 2L.$$

A block diagram illustrating the steps in performing the UT is shown in Fig. 1.

Remark 3.2: Note that this method differs substantially from general Monte Carlo sampling methods which require orders of magnitude more sample points in an attempt to propagate an accurate (possibly non-Gaussian) distribution of the state. The deceptively simple approach taken with the UT results in approximations that are accurate to the third order for Gaussian inputs for all nonlinearities. For non-Gaussian inputs, approximations are accurate to at least the second order, with the accuracy of the third- and higher order moments being determined by the choice of α and β.

III.C. Extension to UT: The UKF

In view of the foregoing, the UKF is an extension of the UT to the following recursive estimation:

$$\hat{x}_k = x_{k_{prediction}} + \kappa_k \left[y_k - y_{k_{prediction}} \right] \quad (25)$$

where the state random variables (RV) is redefined as the concentration of the original state and noise variables: $x_k^a = [x_k^T \quad v_k^t \quad n_k^t]^T$. The UT sigma point selection scheme is then applied to this new augmented state RV to calculate the corresponding sigma matrix, $\mathcal{X}_k^a$. The UKF equations are given below. Note that no explicit calculations of Jacobian or Hessians are necessary to implement this algorithm. Initialize with :

$$
\begin{aligned}
\hat{x}_0 &= \mathsf{E}[x_0], \\
P_0 &= \mathsf{E}[(x_0 - \hat{x}_0)(x_0 - \hat{x}_0)^T], \\
\hat{x}_0^a &= \mathsf{E}[x^a] = [\hat{x}_0^T \quad 0 \quad 0]^T.
\end{aligned}
\quad (26)
$$

For $k \in [1, ..., \infty]$, calculate the sigma points as:

$$\mathcal{X}_{k-1}^a = [\hat{x}_{k-1}^a \quad \hat{x}_{k-1}^a + \gamma\sqrt{P_{k-1}^a} \quad \hat{x}_{k-1}^a - \gamma\sqrt{P_{k-1}^a}] \quad (27)$$

The UKF time-update equations are:

$$
\begin{aligned}
\mathcal{X}_{k|k-1}^x &= \mathsf{F}(\mathcal{X}_{k-1}^x, \quad u_{k-1}, \quad \mathcal{X}_{k-1}^\nu), \\
\hat{x}_k^- &= \sum_{i=0}^{2L} W_i^m \mathcal{X}_{i,k|k-1}^x, \\
P_k^- &= \sum_{i=0}^{2L} W_i^c (\mathcal{X}_{i,k|k-1}^x - \hat{x}_k^-)(\mathcal{X}_{i,k|k-1}^x - \hat{x}_k^-)^T, \\
\mathcal{Y}_{k|k-1} &= \mathbf{H}(\mathcal{X}_{k|k-1}^x, \mathcal{X}_{k-1}^n), \\
\hat{y}_k^- &= \sum_{i=0}^{2L} W_i^m \mathcal{Y}_{i,k|k-1}
\end{aligned}
\quad (28)
$$

The UKF measurement-update equations are:

$$
\begin{aligned}
P_{\bar{y}_k \bar{y}_k} &= \sum_{i=0}^{2L} W_i^c (\mathcal{Y}_{i,k|k-1} - \hat{y}_k^-)(\mathcal{Y}_{i,k|k-1} - \hat{y}_k^-)^T, \\
P_{x_k y_k} &= \sum_{i=0}^{2L} W_i^c (\mathcal{X}_{i,k|k-1} - \hat{x}_k^-)(\mathcal{Y}_{i,k|k-1} - \hat{y}_k^-)^T, \\
\kappa_k &= P_{x_k y_k} P_{\bar{y}_k \bar{y}_k}^{-1}, \\
\hat{x}_k &= \hat{x}_k^- + \kappa_k(y_k - \hat{y}_k^-), \\
P_k &= P_k^- - \kappa_k P_{\bar{y}_k \bar{y}_k} \kappa_k^T
\end{aligned}
\quad (29)
$$

where

$$
\begin{aligned}
x^a &= [x^T \quad v^T \quad n^T]^T, \\
\mathcal{X}^a &= [(\mathcal{X}^x)^T \quad (\mathcal{X}^v)^T \quad (\mathcal{X}^n)^T]^T, and \\
\gamma &= \sqrt{L+\lambda}
\end{aligned}
\quad (30)
$$

In addition, λ is the composite scaling parameter, L is the dimension of the augmented state, R^v is the process-noise covariance, $\Re^n$ is the measurement-noise covariance, and W_i are the weights.

The time-update equations are:

$$
\begin{aligned}
\chi_{k|k-1}^x &= \mathsf{E}(\chi_{k-1}^x, u_{k-1}, \chi_{k-1}^\nu), \\
\hat{x}_k^- &= \sum_{i=0}^{2L} W_i^m \chi_{i,k|k-1}^x, \\
P_k^- &= \sum_{i=0}^{2L} W_i^c (\chi_{i,k|k-1}^x - \hat{x}_k^-)(\chi_{i,k|k-1}^x - \hat{x}_k^-)^T, \\
Y_{k|k-1} &= \mathbf{H}(\chi_{k|k-1}^x, \chi_{k-1}^n), \ \hat{y}_k^- = \sum_{i=0}^{2L} W_i^m \chi_{i,k|k-1}^Y
\end{aligned}
\quad (31)
$$

The measurement-update equations are:

$$
\begin{aligned}
P_{\bar{y}_k \bar{y}_k} &= \sum_{i=0}^{2L} W_i^c (Y_{i,k|k-1} - \hat{y}_k^-)(Y_{i,k|k-1} - \hat{y}_k^-)^T, \\
P_{x_k y_k} &= \sum_{i=0}^{2L} W_i^c (\chi_{i,k|k-1} - \hat{x}_k^-)(Y_{i,k|k-1} - \hat{y}_k^-)^T, \\
\kappa_k &= P_{x_k y_k} P_{\bar{y}_k \bar{y}_k}^{-1}, \ \hat{x}_k = \hat{x}_k^- + \kappa_k(y_k - \hat{y}_k^-), \\
P_k &= P_k^- - \kappa_k P_{\bar{y}_k \bar{y}_k} \kappa_k^T
\end{aligned}
\quad (32)
$$

where $x^a = [x^t \quad v^t \quad n^t]^t$, $\chi^a = [(\chi^x)^t \quad (\chi^v)^t \quad (\chi^n)^t]^t$, $\gamma = \sqrt{L+\lambda}$. In addition, λ is the composite scaling parameter, L is the dimension of the augmented state, $\Re^v$ is the process-noise covariance, $\Re^n$ is the measurement-noise covariance, and W_i are the weights.

III.D. UKF parameter estimation

Parameter estimation involves learning a nonlinear mapping $\mathbf{y}_k = \mathbf{G}(\mathbf{x}_k, \mathbf{w})$, where $\mathbf{w}$ corresponds to the set of known parameters [44]. $\mathbf{G}(.)$ may be a neural network or another parameterized function. The EKF may be used

to estimate the parameters by writing a new state-space representation

$$\mathbf{w}_{k+1} \quad = \quad \mathbf{w}_k + \mathbf{r}_k \qquad (33)$$
$$\mathbf{d}_k \quad = \quad \mathbf{G}(x_k, w_k) + e_k \qquad (34)$$

where $\mathbf{w}_k$ corresponds to a stationary process with identity state transition matrix, driven by noise $\mathbf{r}_k$. The desired output $\mathbf{d}_k$ corresponds to a non-linear observation on $\mathbf{w}_k$. From the optimized perspective, the following prediction error cost is minimized:

$$J(\mathbf{w}) = \sum_{i=1}^{k} [\mathbf{d}_t - \mathbf{G}(\mathbf{x}_t, \mathbf{w})]^T (\mathbf{R}^e)^{-1} [\mathbf{d}_t - \mathbf{x}\mathbf{G}(x_t, w)]$$

$$(35)$$

Thus, if the noise covariance $\mathbf{R}^e$ is a constant diagonal matrix, then, in fact, it cancels out of the algorithm, and hence can be set arbitrarily(e.g., $\mathbf{R}^e = 0.5I$). Alternatively, $\mathbf{R}^e$ can be set to specify a weighted MSE cost. The innovations covariance $\mathbf{E}[\mathbf{r}_k \quad \mathbf{r}_k^T] = \mathbf{R}_k^r$, on the other hand, affects the convergence rate and tracking performance. Roughly speaking, the larger the covariance, the more quickly older data is discarded. There are several options on how to choose $\mathbf{R}_k^r$.
• Set $\mathbf{R}_k^r$ to an arbitrary fixed diagonal value, which may then be "annealed" towards zero as training continues.
• Set $\mathbf{R}_k^r = (\lambda_{RLS}^{-1} - 1)\mathbf{P}_{w_i}$, where $\lambda_{RLS} \ \epsilon \ (0,1]$ is often referred to as the "forgetting factor". This provides for an approximate exponentially decaying weighting on past data. Note that λ_{RLS} should not be confused with λ used for sigma-point calculation.
• Set

$$\mathbf{R}_k^r \quad = \quad (1 - \alpha_{RM})\mathbf{R}_r^{k-1} + \alpha_{RM}\mathbf{K}_k^w [\mathbf{d}_k - \mathbf{G}(\mathbf{x}_k, \hat{\mathbf{w}})]$$
$$\times \quad [\mathbf{d}_k - \mathbf{G}(\mathbf{x}_k, \hat{\mathbf{w}})]^T (\mathbf{K}_k^w)^T$$

which is a Robbins-Monro stochastic approximation scheme for estimating the innovations. The method assumes that the covariance of the Kalman update model is consistent with the actual update model. Typically, $\mathbf{R}_k^r$ is also constrained to be a diagonal matrix, which implies an independence assumption on the parameters. Note that a similar update may also be used for $\mathbf{R}_k^e$.

Remark 3.3: Consider a state-space model given by:

$$\mathbf{x}_t \quad = \quad f(\mathbf{x}_t - 1) + \epsilon, \quad \mathbf{x}_t \in \mathbf{R}^m \qquad (36)$$
$$\mathbf{y}_t \quad = \quad g(\mathbf{x}_t) + \nu, \quad \mathbf{y}_t \in \mathbf{R}^D \qquad (37)$$

Here, the system noise $\epsilon \sim N(0, \Sigma_\epsilon)$ and the measurement noise $\nu \sim N(0, \Sigma_\nu)$ noise are both Gaussian.
The EKF linearizes f and g at the current estimate of $\mathbf{x}_t$ and treats the system as a non-stationary linear system even though it is not. The UKF propagates several estimates of $\mathbf{x}_t$ through f and g and reconstructs a Gaussian distribution assuming the propagated values came from a linear system. Moreover, in non-linear processes, when we are using EKF, the pdf is propagated through a linear approximation of the system around the operating point at each time instant. In doing so,

the EKF needs the Jacobian matrices which may be difficult to obtain for higher order systems, especially in the case of time-critical applications. Further, the linear approximation of the system at a given time instant may introduce errors in the state which may lead the state to diverge over time. In other words, the linear approximation may not be appropriate for some systems. Also in EKF algorithm, during the time-update (prediction) step, the mean is propagated through the nonlinear function, in other words, this introduces an error since in general $\bar{y} \neq g(\bar{\mathbf{x}})$. Whereas, in case of the UKF, during the time-update step, all the sigma points are propagated through the nonlinear function which makes the UKF a better and more effective nonlinear approximator. The UKF principle is simple and easy to implement as it does not require the calculation of Jacobian at each time step. The UKF is accurate up to second order moments in the pdf propagation where as the EKF is accurate up to first order moment [45].

IV. IMPROVED MSDF TECHNIQUE

MSDF method has received major attention for various industrial applications. MSDF can be done at a variety of levels from the raw data or observation level to the feature/state vector level and the decision level. This idea can lead to utilization of different possible configurations or architectures to integrate the data from disparate sensors in an industrial plant to extract the desired monitoring information. Using Kalman filtering as the data fusion algorithm, multiple sensors can be integrated in two key architecture scenarios called centralized method and decentralized or distributed method. These methods have been widely studied over the last decade [46] and [47].

IV.A.I. Centralized integration method

In centralized integration method, all the raw data from different sensors is sent to single location to be fused. This architecture is sometimes called as measurement fusion integration method [46] and [47], in which observations or sensor measurements are directly fuses to obtain a global or combined measurement data matrix H^T. Then, it uses a single Kalman filter to estimate the global state vector based upon the fused measurement. Although this conventional method provides high fusion accuracy to the estimation problem, the large number of states may require high processing data rates that cannot be maintained in practical real time applications. Another disadvantage of this method is the lack of robustness in case of failure in sensor or central filter itself. For these reasons, parallel structures can often provide improved failure detection and correction, enhance redundancy management, and decreased costs for multi-sensor system integration. This method integrates the sensor measurement information as

follows:

$$z(k) = [z_1(k) \ldots z_N(k)]^T \tag{38}$$

$$H(k) = [H_1(k) \ldots H_N(k)]^T \tag{39}$$

$$R(k) = diag[R_1(k) \ldots R_N(k)] \tag{40}$$

where $R_j(k)$ is the covariance matrix.

IV.A.II. Decentralized integration method

As such, there has recently been considerable interest shown in distributed integration method in which the filtering process is divided between some local Kalman filters working in parallel to obtain individual sensor-based state estimates and one master filter combining these local estimates to yield an improved global state estimate. This architecture is sometimes called as state-vector fusion integration method [46] and [47]. The advantages of this method are higher robustness due to parallel implementation of fusion nodes and lower computation load and communication cost at each fusion node. It is also applicable in modular systems where different process sensors can be provided as separate units. On the other hand, distributed fusion is conceptually a lot more complex and is likely to require higher bandwidth compared with centralized fusion. This method integrates the sensor measurement information as follows:

$$z(k) = [\sum_{j=1}^{N} R_j^{-1}(k)]^{-1} \sum_{j=1}^{N} R_j^{-1}(k)z_j(k) \tag{41}$$

$$H(k) = [\sum_{j=1}^{N} R_j^{-1}(k)]^{-1} \sum_{j=1}^{N} R_j^{-1}(k)H_j(k) \tag{42}$$

$$R(k) = [\sum_{j=1}^{N} R_j^{-1}(k)]^{-1} \tag{43}$$

where $R_j(k)$ is the covariance matrix.
In this paper, the architectures are being implemented using UKF as shown in Fig. 2 and Fig. 3 respectively.

V. EVALUATION OF THE PROPOSED SCHEME

The evaluation of the proposed scheme has been made on the following systems:
• A QTS, and
• An IUB.

The following sections show the detailed implementation and simulation of the proposed scheme.

V.A. A QTS model

The process is called as QTS and consists of four inter-connected water tanks and two pumps. Its manipulated variables are voltages to the pumps and the controlled variables are the water levels in the two lower tanks. The QTS presents a multi-input-multi-output system. This
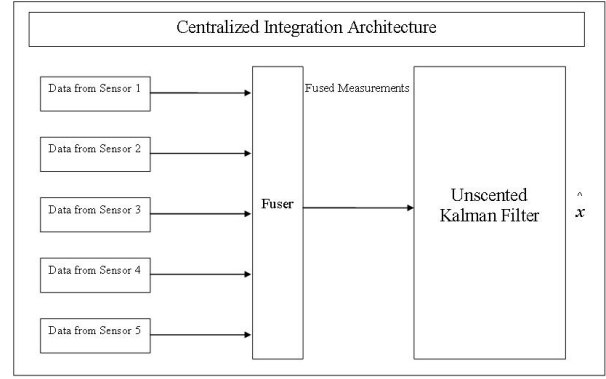

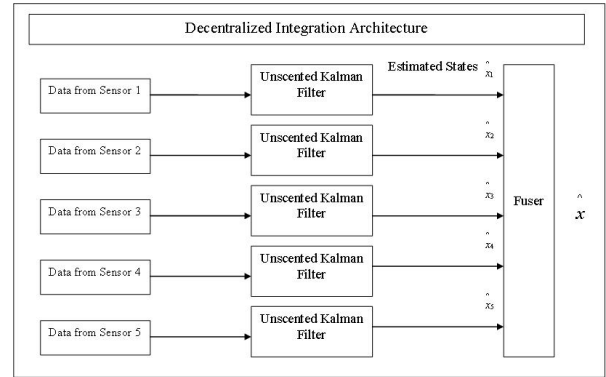Fig. 2. Centralized integration method using Unscented Kalman Filter

Fig. 3. Decentralized integration method using Unscented Kalman Filter

system is a real-life control problem prototyped to experiment on, and try to solve in the most efficient way, since it deals with multiple variables, thus it gives a reflection for the large systems in industry such as petro-chemical plants, waste water treatment plants, liquid level systems etc.
The schematic description of the QTS can be visualized in Fig. 4. The system has two control inputs (pump throughputs) which can be manipulated to control the water level in the tanks. The two pumps are used to transfer water from a sump into four overhead tanks. The two tanks at the upper level drain freely into the two tanks at the bottom level and the liquid levels in these bottom two tanks are measured by pressure sensors. The piping system is designed such that each pump affects the liquid levels of both measured tanks. A portion of the flow from one pump is directed into one of the lower level tanks and the rest is directed to the overhead tank that drains into the other lower level tank. By adjusting the bypass valves of the system, the proportion of the water pumped into different tanks can be changed to adjust the degree of
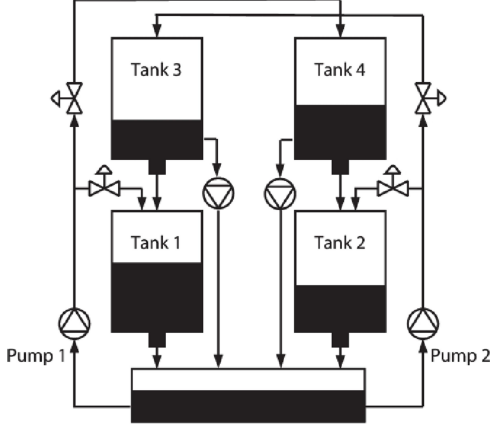
Fig. 4. Schematic diagram of a Quadruple tank system

interaction between the pump throughputs and the water levels. The output of each pump is split into two using a three-way valve. Thus each pump output goes to two tanks, one lower and another upper, diagonally opposite and the ratio of the split up is controlled by the position of the valve. Because of the large water distribution load, the pumps have been supplied 12 V each. The mathematical modeling of the quadruple tank process can be obtained by using Bernoulli's law [48]. The constants are denoted in Table I. A nonlinear mathematical model of the four-tank model is derived based on mass balances and Bernoulli law. Mass balance for one of the tanks is:

$$A\frac{dh}{dt} = q_{in} - q_{out} \tag{44}$$

where A denotes the cross section of the tank, h, q_{in} and q_{out} denote the water level, the inflow and outflow of the tank, respectively. In order to establish a relationship between output and height Bernoulli law is used. It states that

$$q_{out} = a\sqrt{2gh} \tag{45}$$

where a is the cross section of the outlet hole (cm^2) and g is the acceleration due to gravity. A common multiplying factor for an orifice of the type being used in this system is coefficient of discharge k. We can therefore rewrite Bernoulli equation as:

$$q_{out} = ak\sqrt{2gh} \tag{46}$$

The flow through each pump is split so that a proportion of the total flow travels to each corresponding tank. This can be adjusted via one of the two valves shown in Fig. 4. Assuming that the flow generated is proportional to the voltage applied to each pump, (change) v, and that q_T and q_B are the flows going to the top and bottom tanks, respectively, we are able to come up with the following relationships. $q_B = \gamma k\nu$, $q_T = (1-\gamma)k\nu$ where $\gamma \epsilon [0, 1]$.

V.A.I. Fault model of QTS

Combining all the equations for the interconnected four-tank system we obtain the physical system. A fault model can then be constructed by adding extra holes to each tank. The mathematical model of the faulty quadruple tank system can be given as:

$$\frac{dh_1}{dt} = -\frac{a_1}{A_1}\sqrt{2gh_1} + \frac{a_3}{A_1}\sqrt{2gh_3} + \frac{\gamma_1 k_1}{A_1}\nu_1 + \frac{d}{A_1}$$
$$- \frac{a_{leak1}}{A_1}\sqrt{2gh_1}$$
$$\frac{dh_2}{dt} = -\frac{a_2}{A_2}\sqrt{2gh_2} + \frac{a_4}{A_2}\sqrt{2gh_4} + \frac{\gamma_2 k_2}{A_2}\nu_2 - \frac{d}{A_2}$$
$$- \frac{a_{leak2}}{A_2}\sqrt{2gh_2}$$
$$\frac{dh_3}{dt} = -\frac{a_3}{A_3}\sqrt{2gh_3} + \frac{(1-\gamma_2)k_2}{A_3}\nu_2$$
$$- \frac{a_{leak3}}{A_3}\sqrt{2gh_3}$$
$$\frac{dh_4}{dt} = -\frac{a_4}{A_4}\sqrt{2gh_4} + \frac{(1-\gamma_1)k_1}{A_4}\nu_1$$
$$- \frac{a_{leak4}}{A_4}\sqrt{2gh_4}$$
$$\frac{d\nu_1}{dt} = -\frac{\nu_1}{\tau_1} + \frac{1}{\tau_1}u_1$$
$$\frac{d\nu_2}{dt} = -\frac{\nu_2}{\tau_2} + \frac{2}{\tau_2}u_2 \tag{47}$$

Two fault scenarios are created by using the QTS in the simulation program. In these scenarios incipient single and multiple tank faults (i.e., leakages) are created by changing some system parameters manually during the simulation at certain times. The system inputs, outputs and/or some states are corrupted by Gaussian noise with zero mean and standard deviation of 0.1.

a) Scenario I: Leakage fault in tank 1: In this scenario, while the system is working in real time, single incipient fault (i.e., tank 1 leakage percentage), is created by changing the parameter a_{leak1} to $0.81\ cm^2$ (i.e., the value 0.81 is 30 percent of the cross-section of the outlet hole of the tank 1) in the QTS at 350 seconds.

b) Scenario II: Leakage fault in tank 2 and 3: In this scenario, while the system is working in real time, multiple incipient faults (i.e., tank 2 and 3 leakage percentages) are created by changing the parameter a_{leak2} to $1.62\ cm^2$, a_{leak3} to $0.54\ cm^2$ (i.e., the value 1.62 is 60 percent of the cross-section of the outlet holes of the tank 2, and 0.54 is 20 percent of the cross-section of the outlet holes of the tank 3) in the QTS at 350 seconds.

V.A.II. Implementation Structure of UKF

The general elementary implementation structure of UKF on one of the states of the QTS can be described in Table II where the first step is involved towards initializing the parameters and then defining the conditions, the second step defines the states and measurement equations of the

TABLE II
EQUATIONS OF THE GENERAL STRUCTURE IMPLEMENTATION OF UKF

Step 1: Initializing the parameters

$n = 6$;	n: number of states
$q = 0$;	q: standard deviation of process
$r = 1.9$;	r: standard deviation of measurement
$Q = q^2 \times eye\ (n)$; $R = r^2$	Q: covariance of process, R: covariance of measurement

Step 2: Defining the states and measurement equation of the system

$f = @(x)[x(1); x(2); x(3); x(4); x(5); x(6)]$;	f: nonlinear state equations
$h = @\ (x)x(1)$;	h: measurement equation
$s = [0; 0; 1; 0; 1; 1]$;	s: defines the initial state
$x = s+q \times randn(6, 1)$; $P = eye(n)$;	x: initial state with noise, P: initial state covariance
N	N: presents the total dynamic steps

Step 3: Upgrading the estimated parameter under observation

FOR $k = 1 : N$	
$x_1(1); x_2(1); x_3(1); x_4(1); x_5(1); x_6(1)$;	*Initializing,*
H= $[x_1$(k); x_2(k); x_3(k); x_4(k); x_5(k); x_6(k)]	
$z = h(s) + r \times randn$;	(measurements)
$sV\ (:, k) = s$; $zV\ (:, k) = z$;	s: save actual state, z: save measurement
Then injecting the things in the following equation (function)	
$[x, P] = ukf\ (x, P, hmeas, z, Q, R, h)$	*where three functions completing the process of UKF*

Function 1: The UKF

$[\ x, P\ ] = ukf\ (\ x, P, hmeas, z, Q, R, h\ )$	returns state estimate, x and state covariance, P)
NOTE: For nonlinear dynamic system	(for simplicity, noises are assumed as additive)
$x_{k+1} = f\ (x_k)+ w_k$	(where $w \sim$ N(0, Q) meaning w is Gaussian noise with covariance Q)
$z_k = h\ (x_k) + \nu_k$	(where $\nu \sim$ N(0, R) meaning ν is Gaussian noise with covariance R)

INPUTS:
f: function handle for $f(x)$, x: '*a-priori*' *state estimate*
P: '*a-priori*' *estimated state covariance, h: function handle for* h (x)
z: current measurement, Q: process noise covariance
R: measurement noise covariance
OUTPUTS:

x: ' *a-posteriori* ' *state estimate, P:* ' *a-posteriori* ' *state covariance*	
$L = numel\ (x)$;	(where L presents the number of states)
$m = numel\ (z)$;	(where m presents the number of measurements)
$\alpha = 1e^{-3}$; $k_i = 3 - L$; $\beta = 2$	(default, tunable)
$\lambda = \alpha^2 \times (L + k_i - L)$; $c = L + \lambda$;	(scaling factor)
$W_m = (\frac{\lambda}{c} + \frac{0.5}{c} + zeros\ (1, 2 \times L))$;	(weights for means)
$W_c = W_m$; $W_c(1) = W_c(1) + (1 - alpha^2 + \beta)$;	weights for covariance
$c = \sqrt{c}$; $P_1 = P + Q$; $X = sigmas\ (x, P, c)$;	(sigma points around x)
$[\ x_1, X_1, P_1, X2\ ] = ut\ (\ fstate, X, W_m, W_c, L, Q\ )$;	(UT of process)
$X_2 = X - x\ (\ :, ones\ (1, 2 \times L+1\ )\ )$;	
$[\ z_1, Z_1, P_2, Z_2\ ] = ut\ (\ hmeas, X, W_m, W_c, m, R, h\ )$;	(UT of measurements)
$P_{12} = X_2 \times diag\ (\ W_c\ ) \times Z_2^T$;	(transformed cross-covariance)
$R = chol\ (\ P_2\ )$;	(where *chol* presents the Cholesky factorization)
$K = (\ \frac{P_{12}/R}{R^T}\ )$;	(Filter gain)
$K = P_{12} \times inv\ (\ P_2\ )$;	
$x = x + K \times (z\text{-}z_1)$; $P = P_1\text{-}K \times P_{12}^T$;	(state & covariance update respectively)

Function 2: UT — Unscented Transformation

$function\ [\ y, Y, P, Y_1\ ] = ut\ (\ F, X, W_m, W_c, n, R, h\ )$
INPUTS:
f: nonlinear map; X: sigma points; W_m: weights for mean
W_c: weights for covariance; n: number of outputs of f; R: additive covariance
OUTPUTS:
y: transformed mean; Y: transformed sampling points; P: transformed covariance
Y_1: transformed deviations
L=size(X, 2); y=zeros(n, 1); Y=zeros (n, L); x=[h];
FOR k=1: L
Y(k) = $x\ (h)$;
$y = y +W_m$(k) $\times Y$(k);
END
$Y_1 = Y\text{-}\ y$; $P = Y_1 \times$ diag(W_c) $\times Y_1^T$ +R;

Function 3: Sigma Points — Sigma points around reference point

function $X = sigmas\ (\ x, P, c\ )$
INPUTS:
x: reference point; P: covariance; c: coefficient
OUTPUTS:
X: Sigma points; $A = c \times chol\ (\ P^T\ )$;
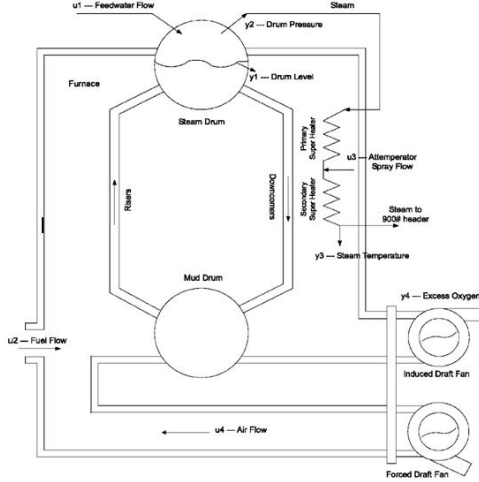$Y = x\ (:, ones(1, numel\ (x)))$; $X = [\ x\ Y + A\ Y\ \text{-}\ A\ ]$;

Fig. 5.   Schematic Diagram of an Industrial Utility Boiler [50]

system. The third step shows the estimated parameter upgrade, which is followed by three functions completing the process of UKF.

V.B. Utility boiler

The utility boilers in Syncrude Canada are water tube drum boilers. Since, steam is used for generating electricity and process applications, demand for steam is variable. The control objective of the co-generation system is to track steam demand while maintaining steam pressure and steam temperature of the header at their respective set-points. In the system, the principal input variables are u_1, feed water flow rate (kg/s); u_2, fuel flow rate (kg/s); and u_3, attemperator spray flow rate (kg/s), the states are x_1, fluid density, x_2, drum pressure, x_3, water flow input, x_4, fuel flow input, x_5, spray flow input. The principal output variables are y_1, drum level (m); y_2, drum pressure kPa; and y_3, steam temperature C^0 [49]. The schematic diagram of the utility boiler can be seen in Fig. 5.

V.B.I. Steam flow dynamics

Steam flow plays an important role in the drum-boiler dynamics. Steam flow from the drum to the header, through the super heaters, is assumed to be a function of the pressure drop from the drum to the header. We use a modified form of the Bernoullis law to represent flow versus pressure, with friction [51]. This expression is written as:

$$q_s = K\sqrt{x_2^2 - P_{header}^2} \qquad (48)$$

where q_s is the steam mass flow rate, K is a constant, and x_2 and P_{header} are the upstream and downstream pressures, respectively. The constant K is chosen to produce agreement between measured flow and pressure

drop at a reference condition. Because, for the real system P_{header}= 6306(kPa), by measuring the steam flow and drum pressure in the real system, the value of K is identified and the steam flow in the system can be modeled as:

$$q_s = 0.03\sqrt{x_2^2 - 6306^2} \qquad (49)$$

V.B.II. Drum pressure dynamics

To model the pressure dynamics, first step identification is done to observe the behavior of the system. By applying step inputs to the three different inputs at different operating points, we observe for a step increase in the feedwater and fuel flow, the system behaves like a first order system with the same time constant. By applying a step to spray flow input, the system behaves like a first order system with different time constant. The dynamics for the drum pressure is chosen as follows:

$$\dot{x}_2 = (c_1 x_2 + c_2)q_s + c_3 u_1 + c_4 u_2 \qquad (50)$$

$$y_2 = x_2 \qquad (51)$$

Finally, the dynamics of the drum pressure can be modeled as:

$$\dot{x}_2 = (-1.8506 \times 10^{-7} x_2 - 0.0024)\sqrt{x_2^2 - (6306)^2}$$
$$-0.0404 u_1 + 3.025 u_2 \qquad (52)$$
$$y_2(t) = x_2(t) + p_0 \qquad (53)$$

where p_0=8.0715, p_0=-0.6449 and p_0=-6.8555 for low, normal and high load, respectively. At the three operating points, the initial conditions are x_{2_0} =6523.6, x_{2_0} =6711.5 and x_{2_0} =6887.9 for low, normal and high load, respectively.

V.B.III. Drum level dynamics

Identification of the water level dynamics is a difficult task. Applying step inputs to the inputs separately, show that the level dynamics is unstable. By increasing the water flow rate, the level increases and by increasing the fuel flow, the level decreases. Three inputs, water flow, fuel flow and steam flow affect on the drum water level. Let x_1, and V_T denote the fluid density and total volume of the system, then we have

$$\dot{x}_1 = \frac{u_1 - q_s}{V_T} \qquad (54)$$

where $V_T = 155.1411$. By doing several experiments, it was observed that the dynamics of the drum level can be given by:

$$y_1 = c_5 x_1 + c_6 q_5 + c_7 u_5 + c_8 u_2 + c_9 \qquad (55)$$

The constants c_i,i= 5, ..., 9 should be identified from the plant data. The initial values of x_1 at the three operating points are given by x_{1_0}= 678.15, x_{1_0}= 667.1, and x_{1_0}= 654.628 for low, normal and high load, respectively.

V.B.IV. Steam temperature

In the utility boiler, the steam temperature must be kept at a certain level to avoid overheating of the super-heaters. To identify a model for steam temperature, first step identification is used. By applying a step to the water flow input, steam temperature increases and the steam temperature dynamics behaves like a fist order system. Applying a step to the fuel flow input, the steam temperature increases and the system behaves like a second order system. Applying a step to the spray flow input, steam temperature decreases and the system behaves like a first order system. Then, a third order system is selected for the steam temperature model. This step identification gives an initial guess for local time constants and gains. By considering steam flow as input and applying input PRBS at the three operating points, local linear models for the steam temperature dynamics are defined. Combining the local linear models, the following nonlinear model is identified for all three operating points with a good fitness.

$$\dot{x}_3(t) = (-0.0211\sqrt{x_2^2 - (6306)^2} + x_4 - 0.0010967u_1$$
$$+0.0475u_2 + 3.1846u_3 \tag{56}$$

$$\dot{x}_4(t) = 0.0015\sqrt{x_2^2 - (6306)^2} + x_5 + 0.001u_1$$
$$+0.32u_2 - 2.9461u_3 \tag{57}$$

$$\dot{x}_5(t) = -1.278 \times 10^{-3}\sqrt{x_2^2 - (6306)^2} - 0.00025831$$
$$x_3 - 0.29747\ x_4 - 0.8787621548\ x_5$$
$$0.00082u_1 - 0.2652778\ u_2 + 2.491\ u_3 \tag{58}$$

$$y_3 = x_3 + T_0 \tag{59}$$

where T_0=443.3579, T_0=446.4321, and T_0=441.9055 for low load, normal load and high load, respectively. At three operating points, we have x_{3_0}=42.2529, x_{4_0}=3.454, x_{5_0}=3.45082, for low load, x_{3_0}=49.0917, x_{4_0}=2.9012, x_{5_0}=2.9862, for normal load, and x_{3_0}=43.3588, x_{4_0}=−0.1347 and x_{5_0}=−0.2509 for high load. Combining the so far achieved results, the identified model for the utility boiler can be obtained. In addition, the following limit constraints exist for the three control variables:

$$0 \leq u_1 \leq 120,\ 0 \leq u_2 \leq 7 \tag{60}$$
$$0 \leq u_3 \leq 10 \tag{61}$$

V.B.V. Fault model for IUB

Fault model for the IUB is being developed. To construct this model extra holes are added to each tank.The mathematical model of the faulty utility boiler can be given as follows where fault of steam pressure are there in state 4 and 5:

$$\dot{x}_1(t) = \frac{u_1 - 0.03\sqrt{x_2^2 - (6306)^2}}{155.1411} \tag{62}$$

$$\dot{x}_2(t) = (-1.8506 \times 10^{-7}x_2 - 0.0024)\sqrt{x_2^2 - (6306)^2}$$
$$-0.0404u_1 + 3.025u_2 \tag{63}$$

$$\dot{x}_3(t) = -0.0211\sqrt{x_2^2 - (6306)^2} + x_4 - 0.0010967u_1$$
$$+0.0475u_2 + 3.1846u_3 \tag{64}$$

$$\dot{x}_4(t) = 0.0015\sqrt{x_2^2 - (6306)^2} + x_5 - 0.001u_1$$
$$+0.32u_2 - 2.9461u_3$$
$$+(a_{st\ pr})\sqrt{x_2^2 - (6306)^2} \tag{65}$$

$$\dot{x}_5(t) = -1.278 \times 10^{-3}\sqrt{x_2^2 - (6306)^2}$$
$$-0.00025831\ x_3 - 0.29747\ x_4$$
$$-0.8787621548\ x_5 - 0.00082\ u_1 - 0.2652778$$
$$u_2 + 2.491\ u_3$$
$$+(a_{st\ pr})\sqrt{x_2^2 - (6306)^2} \tag{66}$$

Two fault scenarios are created by using utility boiler in the simulation program. In these scenarios steam pressure are is added there in state 4 and 5 resulting in a more uncontrolled non-linear system as can be seen Eqn. (65) and Eqn. (66) respectively.

VI. Simulation Results

What follows, we present simulation results for UKF with centralized and decentralized multi-sensor data fusion methods on two dynamical systems:
- QTS and
- IUB

VI.A. QTS

A series of simulation runs was conducted on the QTS to evaluate and compare the effectiveness of the multi-sensor decentralized and centralized integration approaches based on the UKF data fusion algorithm. To perform different set of experiment same fault scenarios have been used as defined.

VI.A.I. QTS: UKF with centralized MSDF

The simulation results of the UKF embedded in the centralized structure of multi-sensor data fusion technique are depicted in Fig. 6, from which it is evident that the centralized structure was able to estimate the fault but there was a considerable offset in the estimation.

VI.A.II. QTS: UKF with decentralized MSDF

The simulation results of the UKF embedded in the decentralized structure of MSDF are depicted in Fig. 7 and Fig. 8, from which it is shown that with an increasing precision accompanied with a more detailed fault picture, decentralized structure was able to estimate the fault in a much better way as compared to centralized architecture.
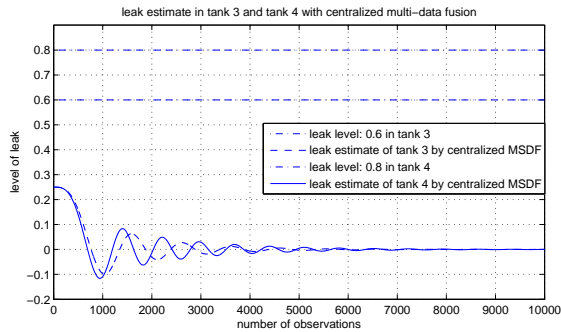
Fig. 6.   Quadruple tank system: Leak Estimate of tank 3 and tank 4 with centralized UKF MSDF approach
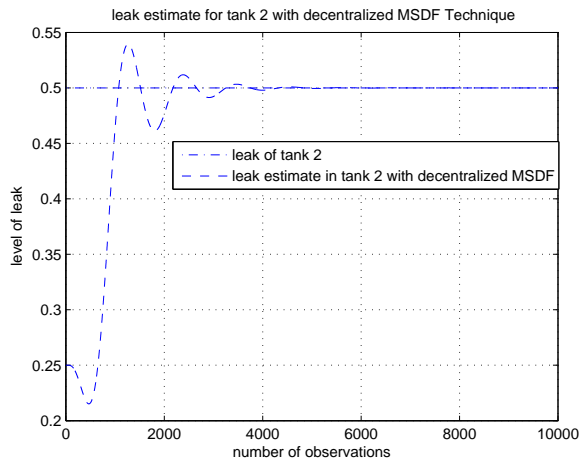

Fig. 7.   Quadruple tank system: Leak Estimate of tank 2 with decentralized UKF MSDF approach. Note: The case is discussing fault estimation and monitoring, had this scheme the case of fault tolerant control, PID controllers and non-linear controllers could have been used for reducing the overshoots, oscillations and steady state values
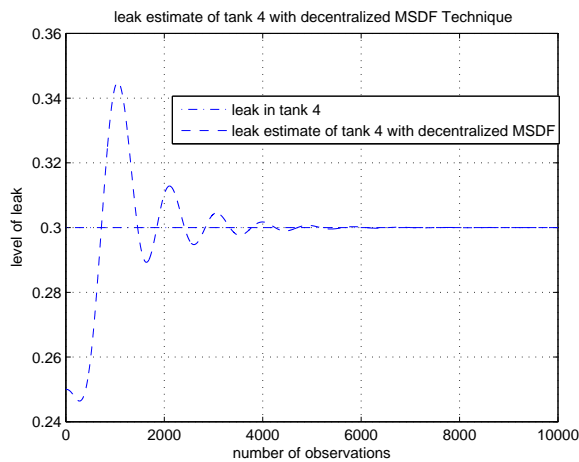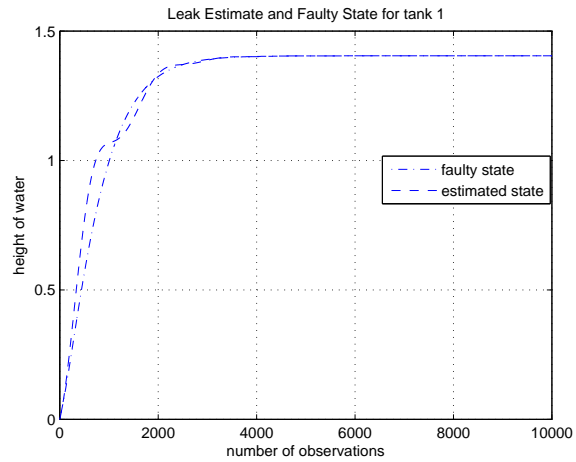

Fig. 8.   Quadruple tank system: Leak Estimate of tank 4 with decentralized UKF MSDF approach. Note: The case is discussing fault estimation and monitoring, had this scheme the case of fault tolerant control, PID controllers and non-linear controllers could have been used for reducing the overshoots, oscillations and steady state values

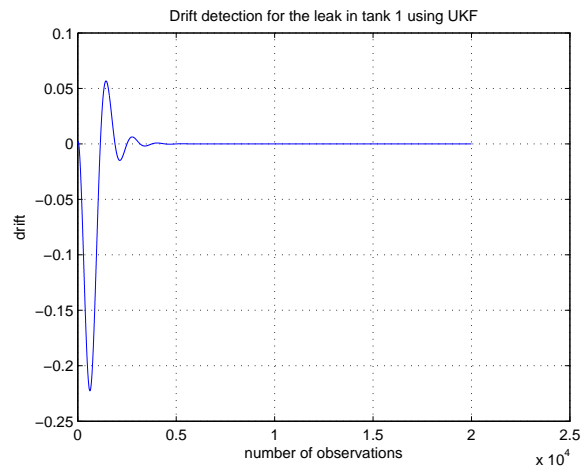Fig. 9.   Quadruple tank system: Leak Estimate and Fault Estimate of tank 1

Fig. 10.   Quadruple tank system: drift detection for the leak in tank 1

VI.A.III. QTS: Drift detection

A fault may occur in any phase and in any part of the plant. Critical faults not detected on time, can lead to adverse effects. In the sequel, the drift detection of the faults using UKF is clarified. It is seen from Fig. 9 that the fault is so incipient that apart from in the beginning, the level of water is achieving the same height. Thus, drift detection can give us a better picture for the fault scenario as shown in Fig. 10. The kinks showing the middle of the height achievement can alarm the engineer about some unusual practice going on in the process.

VI.B. IUB

For assuring the gist of UKF-based fault estimation and monitoring, a series of experiments was also performed on the industrial utility boiler system to evaluate and compare the effectiveness of the multi-sensor decentralized and centralized integration approaches based on the UKF
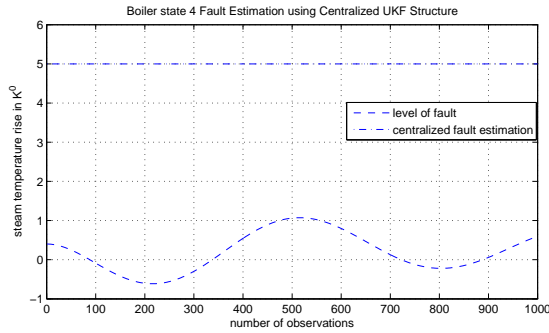
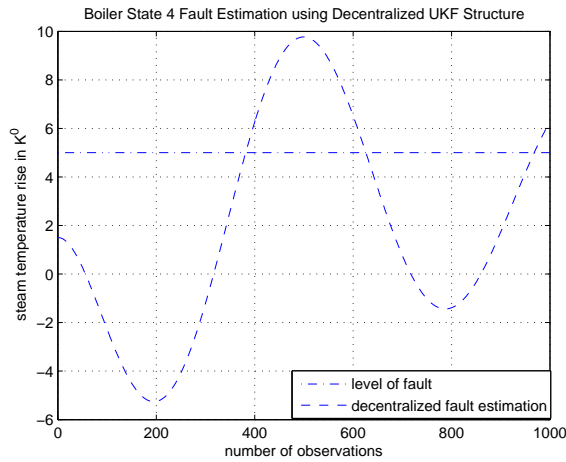Fig. 11.   Utility boiler: estimate of the state 4 using centralized UKF

Fig. 12.   Utility Boiler: estimate of state 4 with decentralized UKF
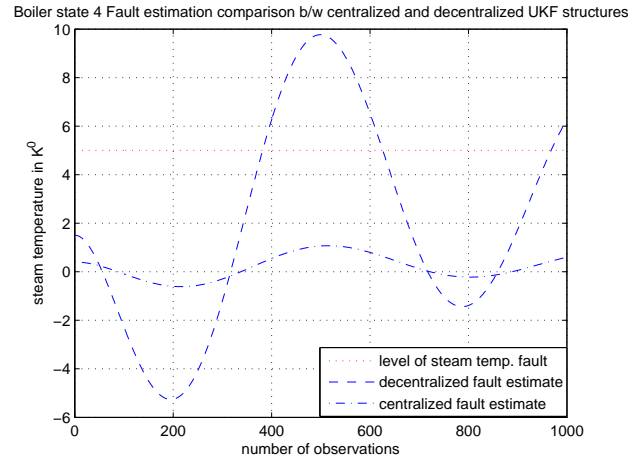

Fig. 13.   Utility Boiler: estimate comparisons
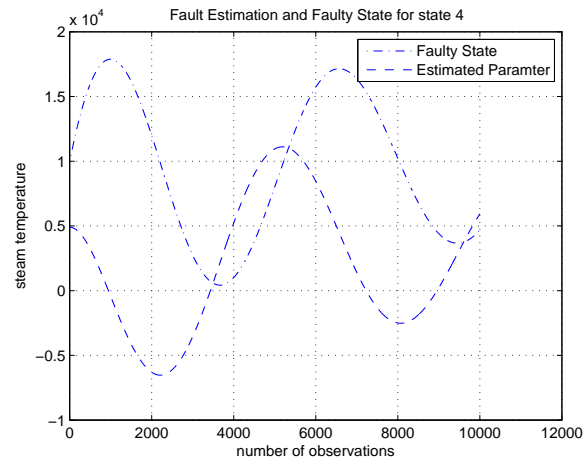
Fig. 14.   Utility boiler: estimated and fault parameters

Fig. 15.   Utility boiler: drift detection

data fusion algorithm. A series of simulation runs was performed with a fault in state 4 and state 5 of the boiler in form of the increased steam temperature.

VI.B.I. IUB: UKF-based centralized MSDF

The simulation results of the UKF embedded in the centralized structure of MSDF technique are depicted in Fig. 11, from which there is a considerable offset in the estimation.

VI.B.II. IUB: UKF-based decentralized MSDF

The results of the UKF embedded in the decentralized structure of MSDF technique can be seen in Fig. 12. The comparison of both centralized and decentralized schemes with the fault estimation is depicted in Fig. 13.

VI.B.III. IUB: UKF-based Drift detection

In IUB, several faults may occur in any part of the boiler. Critical faults not detected on time, can lead to adverse effects. This section shows the drift detection of the faults using UKF. In Fig. 14, the estimated parameter and the fault parameter are shown from which it is seen that there is difference between them despite of the same pattern
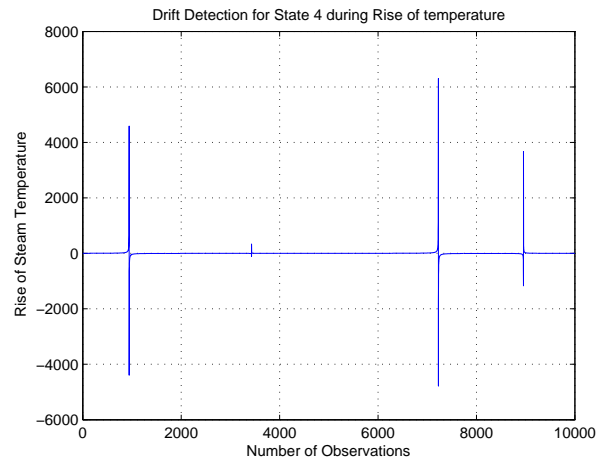
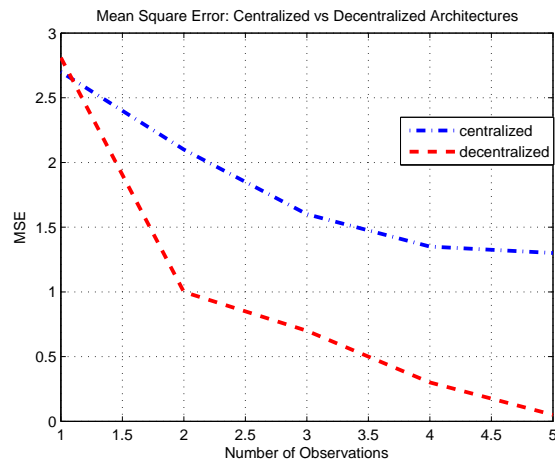Mean Square Error: Centralized vs Decentralized Architectures

Fig. 16. Mean Square Error: Centralized vs Decentralized integration methods

they are following. By drift detection as shown in Fig. 15, we can see the prominent kinks in the profile of the faulty parameter estimation, thus giving sufficient signs for a necessary action.

VI.C. Mean Square error comparison

A mean square error comparison has been made for the centralized and decentralized integration architectures respectively for the particular tank fault estimate. It can be seen from Fig. 16 that mean square error is reduced in less number of iterations for the decentralized integration method as compared to the centralized integration method.

Remark 6.1: In the simulation section, MSDF technique with centralized and decentralized structures of UKF is implemented on the QTS under different leakage fault scenarios and on the IUB with uncontrolled steam pressure fault scenario. It has been shown that in case of both physical systems i.e. QTS and IUB, decentralized structure showing better results than centralized structure, followed by the drift detection which has been made effectively showing prominent kinks of fault. The effectiveness of the decentralized structure in case of IUB was less as compared to QTS, because of large fault of steam pressure introduced in state 4 and state 5 respectively and more nonlinear nature of the model.

VII. CONCLUSION

In this paper, a complete fault estimation and monitoring scheme has been developed by integrating the techniques of MSDF and centralized and decentralized architectures for providing quality reports and ensuring reliable fault detection and it has been made effective by using a deterministic sampling approach known as UKF, thus cap-

turing the posterior mean and covariance accurately complete the overall diagnostic picture. It has been demonstrated that this approach can be used for a reliable detection of incipient faults, which in turn leads to an efficient and cost-effective preventive maintenance scheme. The major contributions of the paper is the implementation of the integrated centralized and decentralized architectures of multi-sensor data fusion and implemented thoroughly on QTS and IUB to achieve both accuracy and reliability of the fault monitoring schemes. The major contribution of the paper is the use of UKF in the integrated design framework of multi-sensor data fusion using centralized and decentralized structures respectively, and comparison of these structures by implementing them on two physical systems.

APPENDIX

REFERENCES

[1] Doguc, O., and Marquez, J. E., 'An efficient fault diagnosis method for complex system reliability', *Proc. 7th Annual Conference on Systems Engineering Research (CSER 2009)*, 2009.

[2] Brambilla, D., Capisani, L. M., Ferrara, A., and Pisu, P., 'Fault detection for robot manipulators via second-order sliding modes', *IEEE Trans. Ind. Electron.*, vol. 55(11), pp. 3954–3963, 2008.

[3] Cusido, J., Romeral, L., Ortega, J. A., Rosero, J. A., Espinosa, A., 'Fault detection in induction machines using power spectral density in wavelet decomposition', *IEEE Trans. Ind. Electron.*, vol. 55(2), pp. 633–643, 2008.

[4] Arogeti, S. A., Wang, D., Low, C. B., 'Mode identification of hybrid systems in the presence of fault', *IEEE Trans. Ind. Electron.*, vol. 57(4), pp. 1452–1467, 2010.

[5] Lezana, P., Pou, J., Meynard, T. A., Rodriguez, J., Ceballos, S., and Richardeau, F., 'Survey on fault operation on multi-level inverters', *IEEE Trans. Ind. Electron.*, vol. 57(7), pp.2207–2218, 2010.

[6] Morgan, I., Liu, H., Tormos, B., and Sala, A., 'Detection and diagnosis of incipient faults in heavy-duty diesel engines', *IEEE Trans. Ind. Electron.*, vol. 57(10), pp. 3522–3532, 2010.

[7] Poncelas, O., Rosero, J. A., Cusido, J., Ortega, J. A., and Romeral, L., 'Motor fault detection using a rogowski sensor without an integrator', *IEEE Trans. Ind. Electron.*, vol. 56(10), pp. 4062–4070, 2009.

[8] Rothenhagen, K., and Fuchs, F. W., 'Current sensor fault detection, isolation, and reconfiguration for doubly fed induction generator', *IEEE Trans. on Ind. Electron.*, vol. 56(10), pp. 4239–4245, 2009.

[9] Hameed, I. A., 'Using the extended Kalman filter to improve the efficiency of greenhouse climate control', *Int. J. Innovative Computing, Information and Control*, vol. 6(6), pp. 2671–2680, 2010.

[10] Palangi, H., and Refan, M. H., 'Error reduction of a low cost GPS receiver for kinematic applications based on a new Kalman filtering algorithm', *Int. J. Innovative Computing, Information and Control*, vol. 6(8), pp. 3775–3786, 2010.

[11] Ohsumi, A., Kimura, T., and Kono, M., 'Kalman filter-based identification of unknown exogenous input of stochastic linear systems via pseudo measurement approach', *Int J. Innovative Computing, Information and Control*, vol. 5(1), pp. 1–16, 2009.

[12] Jun, S., Yang, M., Yao, X., and Zhong, R., 'A new two-stage Kalman filter method for chaos system', *ICIC Express Letters*, vol. 4(2), pp. 539–546, 2010.

[13] Lu, C. L., Chung, N. Y., Lin, C. M., Yu, C. C., and Chen, T. R., 'Applying Kalman filter-based fusion algorithm to estimation problems', *ICIC Express Letters*, vol. 4(6-A), pp.2109–2114, 2010.

[14] Sanchez, M. P., Guasp, M. R., Folch, J. R., Daviu, J. A. A., Cruz, J. P., Panadero, R. P., 'Diagnosis of induction motor faults in time-varying conditions using the polynomial-phase transform of the current', *IEEE Trans. Ind. Electron.*, vol. 58(4), pp. 1428–1439, April 2011.

[15] Wolbank, T. M., Nussbaumer, P., Chen, H., Macheiner, P. E., 'Monitoring of rotor-bar defects in inverter-fed induction machines at zero load and speed', *IEEE Trans. on Ind. Electron.*, vol. 58(5), pp. 1468–1478, May 2011.

[16] Bianchini, C., Immovilli, F., Cocconcelli, M., Rubini, R., Bellini, A., 'Fault detection of linear bearings in brushless AC linear motors by vibration analysis', *IEEE Trans. Ind. Electron.*, vol. 58(5), pp. 1684–1694 , May 2011.

[17] Henao, H., Fatemi, S. M J. R., Capolino, G. A., Sieg-Zieba, S., 'Wire rope fault detection in a hoisting winch system by motor torque and current signature analysis', *IEEE Trans. Ind. Electron.*, vol. 58(5), pp. 1707–1717 , May 2011.

[18] Salahshoor, K., Mosallei, M., and Bayat, M. R., 'Centralized and decentralized process and sensor fault monitoring using data fusion based on adaptive extended Kalman filter algorithm', *J. Measurement*, vol. 41, pp. 1059–1076, 2008.

[19] Isermann, R., 'Model-based fault-detection and diagnosis-status and applications', *Annual Reviews in Control*, vol. 29, pp. 71–85, 2005.

[20] Chow, E. Y., Willsky, A. S., 'Analytical redundancy and the design of robust failure detection systems', *IEEE Trans. Automat. Control.*, vol. 29(7), pp. 603–614, 1984.

[21] Gertler, J. J., *Fault detection and diagnosis in engineering systems*, CRC Press, New York, 484 pages, 1998.

[22] Frank, P. M., Ding, S. X., and Seliger, B. K., 'Current developments in the theory of FDI', *Proc. IFAC Symposium on Fault Detection, Supervision and Safety of Technical Processes*, Budapest, Hungary, vol. 1, pp. 16–27, 2000.

[23] Rahim, M. A., Khalid, H. M., Akram, M., Khoukhi, A., Cheded, L., and Doraiswami, R., 'Quality monitoring and fault detection of a closed-loop system with parametric uncertainties and external disturbances', *Int. J. Advance Manufacturing and Technology*, vol. 55(1–4), pp. 293–306, 2011.

[24] Simani, S., Fantuzzi, C., and Patton, R., 'Model-based fault diagnosis in dynamic systems using identification techniques', *Advances in Industrial Control*, Springer, 2003.

[25] Zhang, G. Q. P., 'Neural networks for classification: a survey', *IEEE Trans. Systems, Man and Cybernetics: Part C-Applications and Reviews*, vol. 30(4), pp. 451–462, 2000.

[26] Wang, Y., Chan, C. W., and Cheung, K. C., 'Intelligent fault diagnosis based on neuro-fuzzy networks for nonlinear dynamic systems', *Proc. IFAC Conference on New Technologies for Computer Control*, Hong Kong, China, pp. 101–104, 2001.

[27] Watanabe, K., Matsura, I., Abe, M., Kubota, M., and Himmelblau, D. M., 'Incipient fault diagnosis of chemical processes via artificial neural networks', *AICHE J.*, vol. 35(11), pp. 1803–1812, 1989.

[28] Venkatasubramanian, V., and Chan, K., 'A neural network methodology for process fault diagnosis', *AICHE J.*, vol. 35(12), pp. 1993–2002, 1989.

[29] Ungar, L. H., Powell, B. A., and Kamens, S. N., 'Adaptive networks for fault diagnosis and process control', *Computers and Chem. Eng.*, vol. 14(4-5), pp. 561–572, 1990.

[30] Venkatasubramanian, V., Vaidyanathan, R., and Yamamoto, Y., 'Process fault detection and diagnosis using neural networks: Steady state processes', *Computers and Chem. Eng.*, vol. 14(7), pp. 699–712, 1990.

[31] Miguel, L. J., and Blazquez, L. F., 'Fuzzy logic-based decision-making for fault diagnosis in a DC motor', *Engineering Applications of Artificial Intelligence*, vol. 18(4), pp. 423–450, 2005.

[32] 'Special section on motor fault detection and diagnosis, *IEEE Trans. Ind. Electron.*, vol. 47(5), pp. 982–1107, 2000.

[33] Ramesh, T. S., Davis, J. F., and Schwenzer, G. M., 'Knowledge-based diagnostic systems for continuous process operations based upon the task framework', *Computers and Chem. Eng.*, vol. 16(2), pp. 109–127, 1992.

[34] Venkatasubramanian, V., 'CATDEX, knowledge-based systems in process engineering: Case studies in heuristic classification', *Technical Report, The CACHE Corporation*, Austin, TX, 1989.

[35] Mehranbod, N., 'A probabilistic approach for sensor fault detection and identification', *Ph.D Dissertation*, Faculty of Drexel University, November 2002.

[36] Kirch, H., Kroschel, K., 'Applying Bayesian networks to fault diagnosis', *Proc. IEEE Conference on Control Applications*, 895, 1994.

[37] Guzman, C. R., Kramer, M., 'GALGO: A genetic algorithm decision support tool for complex uncertain systems modeled with Bayesian belief networks', *Proc. 9th Conf. on Uncertainty in Artif. Intell. (UAI-93)*, San Francisco, pp. 368–375, 1993.

[38] Santoso, N., Darken, C., and Povh, G., 'Nuclear plant fault diagnosis using probabilistic reasoning', *Power Engineering Society Summer Meeting, IEEE*, vol. 2, pp. 714–719, 1999.

[39] Nicholson, A., Brady, J., 'Dynamic belief networks for discrete monitoring', *IEEE Trans. Systems, Man, and Cybernetics*, vol. 24(11), pp. 1593–1610, 1994.

[40] Nicholson, A., 'Fall diagnosis using dynamic belief networks', *Proceedings of the 4th Pacific Rim International Conference on Artificial Intelligence (PRICAI-96)*, vol. 1114 of Lecture Notes in Computer Science, Springer, pp. 206–217, 1996.

[41] Bin Zhang, C., Sconyers, C., Byington, R., Patrick, M. E., Orchard, G., Vachtsevanos, 'A probabilistic fault detection approach: Application to bearing fault detection', *IEEE Trans. Ind. Electron.*, vol. 58(5), pp. 2011–2018, May 2011.

[42] Wan, E. A., Merwe, R. V., and Nelson, A. T., 'Dual estimation and the unscented transformation', in *Advances in Neural Information Processing Systems*, Solla, S. A., Leen, T. K., and Miller, K. R., Eds., Cambridge, MA: MIT Press, pp. 666–672, 2000.

[43] Julier, S. J., J. K. Uhlmann, and H. Durrant-Whyte, 'A new approach for filtering nonlinear systems', *Proc. American Control Conference*, pp. 1628–1632, 1995.

[44] Julier, S. J., and Uhlmann, J. K., 'A new extension of the Kalman filter to nonlinear systems', *Proc. Aero Sense: The 11th Int. Symposium on AeroSpace/Defense Sensing, Simulation and Controls*, vol. 3068, pp. 182–193, 1997.

[45] Van der Merwe, R., 'Sigma-point Kalman filters for probability inference in dynamic state-space models', *PhD Thesis*, Oregon Health and Science University, 2004.

[46] Gan, Q., and Harris, C. J., 'Comparison of two measurement fusion methods for Kalman filter-based multi-sensor data fusion', *IEEE Trans. Aerospace Electr. Systems*, vol. 37(1), pp. 273–280, 2001.

[47] Harris, C., Hong, X., and Gan, Q., 'Adaptive modeling, estimation and fusion from data: A neurofuzzy approach', Springer, 339 pages, 2002.

[48] Dai, L., Astrom, K., 'Dynamic matrix control of a quadruple tank process', *Proceedings of the 14th IFAC*, 1999, pp. 295–300.

[49] Tan, W., Marquez, H. J., Chen, T., 'Multivariable robust controller design for a boiler system', *IEEE Trans. Control Systems Technology* vol. 10(5), 2002, pp. 735–742.

[50] Marquez, H., Riaz, M., 'Robust state observer design with application to an industrial boiler system', *Control Engineering Practice*, vol. 13, 2005, pp. 713–728.

[51] Perry, R. H., Green, D. W., 'Perrys chemical engineers handbook', *seventh ed.*, McGraw-Hill, 1997.